Article:

collaboration, L, Aaij, R, Adeva, B et al. (795 more authors) (2018) Search for excited B_c^+ states. Journal of High Energy Physics, 2018. 138. ISSN 1126-6708

https://doi.org/10.1007/JHEP01(2018)138

Published for SISSA by Springer

Received: December 13, 2017
Revised: January 15, 2018
Accepted: January 18, 2018
Published: January 29, 2018

Search for excited B_c^+ states

The LHCb collaboration

E-mail: liupan.an@cern.ch

Abstract: A search is performed in the invariant mass spectrum of the $B_c^+\pi^+\pi^-$ system for the excited B_c^+ states $B_c(2^1S_0)^+$ and $B_c(2^3S_1)^+$ using a data sample of pp collisions collected by the LHCb experiment at the centre-of-mass energy of $\sqrt{s} = 8\,\text{TeV}$, corresponding to an integrated luminosity of $2\,\text{fb}^{-1}$. No evidence is seen for either state. Upper limits on the ratios of the production cross-sections of the $B_c(2^1S_0)^+$ and $B_c(2^3S_1)^+$ states times the branching fractions of $B_c(2^1S_0)^+ \to B_c^+\pi^+\pi^-$ and $B_c(2^3S_1)^+ \to B_c^{*+}\pi^+\pi^-$ over the production cross-section of the B_c^+ state are given as a function of their masses. They are found to be between 0.02 and 0.14 at 95% confidence level for $B_c(2^1S_0)^+$ and $B_c(2^3S_1)^+$ in the mass ranges $[6830, 6890]\,\text{MeV}/c^2$ and $[6795, 6890]\,\text{MeV}/c^2$, respectively.

Keywords: B physics, Hadron-Hadron scattering (experiments), Spectroscopy

ArXiv ePrint: 1712.04094

https://doi.org/10.1007/JHEP01(2018)138

JHEP01(2018)138

Contents

1 Introduction	**1**
2 Detector and simulation	**2**
3 Event selection	**3**
4 Upper limits	**5**
5 Summary	**10**
The LHCb collaboration	**13**

JHEP01(2018)138

1 Introduction

The B_c meson family is unique in the Standard Model, as its states contain two different heavy-flavour valence quarks. It has a rich spectroscopy, predicted by various models [1–14] and lattice QCD [15]. The ground state of the B_c meson family, the B_c^+ meson, was first observed by the CDF experiment [16, 17] at the Tevatron collider in 1998.[1] Recently, the ATLAS collaboration reported observation of an excited B_c state with a mass of $6842 \pm 4\,(\text{stat}) \pm 5\,(\text{syst})\,\text{MeV}/c^2$ [18]. Since the production cross-section of the $B_c(2^3S_1)^+$ state is predicted to be more than twice that of the $B_c(2^1S_0)^+$ state [8, 13, 19, 20], the most probable interpretation of the single peak is either a signal for $B_c(2^3S_1)^+ \to B_c^{*+}\pi^+\pi^-$, followed by $B_c^{*+} \to B_c^+\gamma$ with a missing low-energy photon, or an unresolved pair of peaks from the decays $B_c(2^1S_0)^+ \to B_c^+\pi^+\pi^-$ and $B_c(2^3S_1)^+ \to B_c^{*+}\pi^+\pi^-$.[2] The $B_c(2^1S_0)^+$ and $B_c(2^3S_1)^+$ states are denoted as $B_c(2S)^+$ and $B_c^*(2S)^+$ hereafter, and $B_c^{(*)}(2S)^+$ denotes either state.

In the present paper, the $B_c(2S)^+$ and $B_c^*(2S)^+$ mesons are searched for using pp collision data collected by the LHCb experiment at $\sqrt{s} = 8\,\text{TeV}$, corresponding to an integrated luminosity of $2\,\text{fb}^{-1}$. The $B_c(2S)^+$ and $B_c^*(2S)^+$ mesons are reconstructed through the decays $B_c(2S)^+ \to B_c^+\pi^+\pi^-$ and $B_c^*(2S)^+ \to B_c^{*+}\pi^+\pi^-$ with $B_c^{*+} \to B_c^+\gamma$, $B_c^+ \to J/\psi\,\pi^+$ and $J/\psi \to \mu^+\mu^-$. The branching fraction of the $B_c^{(*)}(2S)^+ \to B_c^{(*)+}\pi^+\pi^-$ decay, $\mathcal{B}(B_c^{(*)}(2S)^+ \to B_c^{(*)+}\pi^+\pi^-)$, is predicted to be between 39% and 59% [8, 13]. The low-energy photon in the $B_c^*(2S)^+$ decay chain is not reconstructed. The $B_c^*(2S)^+$ state

[1] Sums over charge-conjugated modes are implied throughout this paper.

[2] The spectroscopic notation $n^{2s+1}L_J$ is used, where n is the radial quantum number, s the total spin of the two valence quarks, L their relative angular momentum (S implies $L = 0$), and J the total angular momentum of the system, *i.e.* spin of the excited state. B_c^{*+} denotes the $B_c(1^3S_1)^+$ state.

still appears in the invariant mass $M(B_c^+\pi^+\pi^-)$ spectrum as a narrow mass peak [20, 21], which is centered at $M(B_c(2S)^+) - \Delta M$, where

$$\Delta M \equiv \left[M(B_c^{*+}) - M(B_c^+)\right] - \left[M(B_c^*(2S)^+) - M(B_c(2S)^+)\right], \tag{1.1}$$

and $M(B_c^+)$ is the known mass of B_c^+. According to theoretical predictions [1–11], the mass of the $B_c(2S)^+$ state, $M(B_c(2S)^+)$, is expected to be in the range $[6830, 6890]\,\mathrm{MeV}/c^2$, and ΔM in the range $[0, 35]\,\mathrm{MeV}/c^2$, such that the peak position of the $B_c^*(2S)^+$ state in $M(B_c^+\pi^+\pi^-)$ is expected to be in the range $[6795, 6890]\,\mathrm{MeV}/c^2$.

2 Detector and simulation

The LHCb detector [22, 23] is a single-arm forward spectrometer covering the pseudorapidity range $2 < \eta < 5$, designed for the study of particles containing b or c quarks. The detector includes a high-precision tracking system consisting of a silicon-strip vertex detector surrounding the pp interaction region, a large-area silicon-strip detector (TT) located upstream of a dipole magnet with a bending power of about 4 Tm, and three stations of silicon-strip detectors and straw drift tubes placed downstream of the magnet. The tracking system provides a measurement of momentum, p, of charged particles with a relative uncertainty that varies from 0.5% at low momentum to 1.0% at 200 GeV/c. The minimum distance of a track to a primary vertex (PV), the impact parameter (IP), is measured with a resolution of $(15 + 29/p_{\mathrm{T}})\,\mu\mathrm{m}$, where p_{T} is the component of the momentum transverse to the beam, in GeV/c. Different types of charged hadrons are distinguished using information from two ring-imaging Cherenkov detectors. Photons, electrons and hadrons are identified by a calorimeter system consisting of scintillating-pad and preshower detectors, an electromagnetic calorimeter and a hadronic calorimeter. Muons are identified by a system composed of alternating layers of iron and multiwire proportional chambers. The online event selection is performed by a trigger, which consists of a hardware stage, based on information from the calorimeter and muon systems, followed by a software stage, which applies a full event reconstruction. At the hardware stage, events are required to have at least one muon with high p_{T} or a hadron with high transverse energy. At the software stage, two muon tracks or three charged tracks are required to have high p_{T} and to form a secondary vertex with a significant displacement from the interaction point.

In the simulation, pp collisions are generated using Pythia 6 [24] with a specific LHCb configuration [25]. The generator Bcvegpy [19] is used to simulate the production of B_c mesons. Decays of hadronic particles are described by EvtGen [26], in which final-state radiation is generated using Photos [27]. The interaction of the generated particles with the detector, and its response, are implemented using the Geant4 toolkit [28] as described in ref. [29]. In the default simulation, the masses of the excited B_c states are set as $M(B_c(2S)^+) = 6858\,\mathrm{MeV}/c^2$, $M(B_c^*(2S)^+) = 6890\,\mathrm{MeV}/c^2$ and $M(B_c^{*+}) = 6342\,\mathrm{MeV}/c^2$, corresponding to $\Delta M = 35\,\mathrm{MeV}/c^2$, and the $B_c^*(2S)^+$ state is assumed to be produced unpolarised. Simulated samples with different mass settings, which cover the expected mass range of the $B_c^{(*)}(2S)^+$ states, are generated to study variations in the reconstruction efficiency.

3 Event selection

To select $B_c^+ \to J/\psi\pi^+$ decays, J/ψ candidates are formed from pairs of opposite-charge tracks. The tracks are required to have p_{T} larger than $0.55\,\mathrm{GeV}/c$ and good track-fit quality, to be identified as muons, and to originate from a common vertex. Each J/ψ candidate with an invariant mass between $3.04\,\mathrm{GeV}/c^2$ and $3.14\,\mathrm{GeV}/c^2$ is combined with a charged pion to form a B_c^+ candidate. The pion is required to have $p_{\mathrm{T}} > 1.0\,\mathrm{GeV}/c$ and good track-fit quality. The J/ψ candidate and the charged pion are required to originate from a common vertex, and the B_c^+ candidates must have a decay time larger than 0.2 ps. Each of the particles is associated to the PV that has the smallest χ^2_{IP}, where χ^2_{IP} is defined as the difference in the vertex-fit χ^2 of a given PV reconstructed with and without the particle under consideration. The χ^2_{IP} of the B_c^+ (π^+) candidate is required to be < 25 (> 9) with respect to the associated PV of the B_c^+ candidate. To further suppress background, a requirement on a boosted decision tree (BDT) [30, 31] classifier is applied. The BDT classifier uses information from the χ^2_{IP} of the two muons, the pion, the J/ψ, and the B_c^+ mesons with respect to the associated PV; the p_{T} of both muons, the J/ψ and π^+ mesons; and the decay length, decay time, and the vertex-fit χ^2 of the B_c^+ meson. The BDT is trained with signal events taken from simulation and background events from the upper sideband containing B_c^+ candidates with masses in the range $[6370, 6600]\,\mathrm{MeV}/c^2$. The distributions of the BDT response for the simulation and the background subtracted data are in agreement. The criterion on the BDT output is chosen to maximise the figure of merit $S/\sqrt{S+B}$, where S and B are the expected numbers of signal and background in the range $M(J/\psi\pi^+) \in [6251, 6301]\,\mathrm{MeV}/c^2$. The mass of the J/ψ candidates is constrained to the known value [32] to improve the B_c^+ mass resolution.[3] The B_c^+ signal yield is obtained by performing an unbinned extended maximum likelihood fit to the $M(J/\psi\pi^+)$ mass distribution, as shown in figure 1. The signal component is modelled by a Gaussian function with asymmetric power-law tails as determined from simulation. The mean and resolution of the Gaussian function are free parameters in the fit. The combinatorial background is described with an exponential function. The contamination from the Cabibbo-suppressed channel $B_c^+ \to J/\psi K^+$, with the kaon misidentified as a pion, is described by a Gaussian function with asymmetric power-law tails. The parameters are also fixed from simulation, with only the Gaussian mean related to the $B_c^+ \to J/\psi\pi^+$ signal as a free parameter to account for the possible small mass difference in data and simulation. The signal yield of B_c^+ decays is determined to be 3325 ± 73.

To reconstruct the $B_c^{(*)}(2S)^+$ states, the B_c^+ candidates with $M(J/\psi\pi^+) \in [6200, 6340]\,\mathrm{MeV}/c^2$ are combined with two opposite-charge tracks. The tracks are required to have $p_{\mathrm{T}} > 0.25\,\mathrm{GeV}/c$, momenta larger than $2\,\mathrm{GeV}/c$ and good track-fit quality, and to be identified as pions. The $B_c^{(*)}(2S)^+$ candidates are required to have good $B_c^+\pi^+\pi^-$ vertex-fit quality. To improve the $B_c^{(*)}(2S)^+$ mass resolution, the mass of B_c^+ candidates is constrained to the known B_c^+ mass [34], and the reconstructed $B_c^{(*)}(2S)^+$ mesons are

[3] The J/ψ mass is taken to be $3096.916\,\mathrm{MeV}/c^2$ according to the 2014 edition of the Review of Particle Physics [32], rather than $3096.900\,\mathrm{MeV}/c^2$ in the 2016 edition [33]. The effect of this choice on the final result is negligible.

JHEP01(2018)138

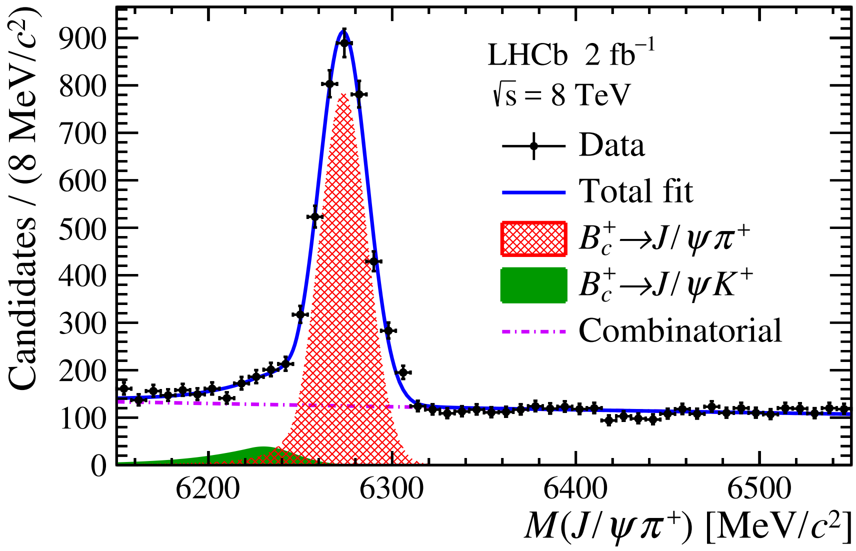

Figure 1. Invariant mass distribution of the selected $B_c^+ \to J/\psi \pi^+$ candidates. The points with error bars represent the data. The blue solid line is the fit to data. The red cross-hatched area shows the signal. The green shaded area represents the $B_c^+ \to J/\psi K^+$ background. The violet dash-dotted line is the combinatorial background.

constrained to originate from the associated PV. To optimise the sensitivity of the analysis, a selection based on a multilayer perceptron (MLP) [35] classifier is applied. To distinguish the signal candidates from combinatorial background, the MLP classifier uses information on the angles between the B_c^+ and π^+, B_c^+ and π^-, and π^+ and π^- candidate momenta projected in the plane transverse to the beam axis; the angles between the $B_c^{(*)}(2S)^+$ momentum and the B_c^+, π^+, and π^- momenta in the $B_c^{(*)}(2S)^+$ centre-of-mass frame; the minimum cosine value of the angles between the momentum of the B_c^+ meson or of one of the pions from $B_c^{(*)}(2S)^+$ and the momentum of the muons or pion from the B_c^+ meson; and the vertex-fit χ^2 of the $B_c^{(*)}(2S)^+$ meson. In simulation, these variables have similar distributions for the $B_c(2S)^+ \to B_c^+\pi^+\pi^-$ and $B_c^*(2S)^+ \to B_c^{*+}(\to B_c^+\gamma)\pi^+\pi^-$ decays. Therefore, the combination of the simulated candidates for the decays $B_c(2S)^+ \to B_c^+\pi^+\pi^-$ and $B_c^*(2S)^+ \to B_c^{*+}(\to B_c^+\gamma)\pi^+\pi^-$ is used as signal for the MLP training, and the background sample consists of the candidates in the lower and upper sidebands of the $M(B_c^+\pi^+\pi^-)$ mass spectrum in data, with $M(B_c^+\pi^+\pi^-) \in [6555, 6785]\,\mathrm{MeV}/c^2$ and $[6900, 7500]\,\mathrm{MeV}/c^2$, respectively. The MLP response is transformed to make the signal candidates distributed evenly between zero and unity, and the background candidates cluster near zero. Only the candidates with transformed output values smaller than 0.02 are rejected, retaining 98% of the signal. The remaining candidates are divided into four categories with the MLP response falling in $(0.02, 0.2)$, $[0.2, 0.4)$, $[0.4, 0.6)$ and $[0.6, 1.0]$, respectively. The $M(B_c^+\pi^+\pi^-)$ distributions in the expected signal region for the four MLP categories are shown in figure 2. The mass resolutions on $M(B_c^+\pi^+\pi^-)$ for the $B_c^{(*)}(2S)^+$ state, $\sigma_{\mathrm{w}}(B_c^{(*)}(2S)^+)$, can be determined from the simulated samples of the $B_c(2S)^+ \to B_c^+\pi^+\pi^-$ and $B_c^*(2S)^+ \to B_c^{*+}(\to B_c^+\gamma)\pi^+\pi^-$ decays. The differences between the mass resolutions

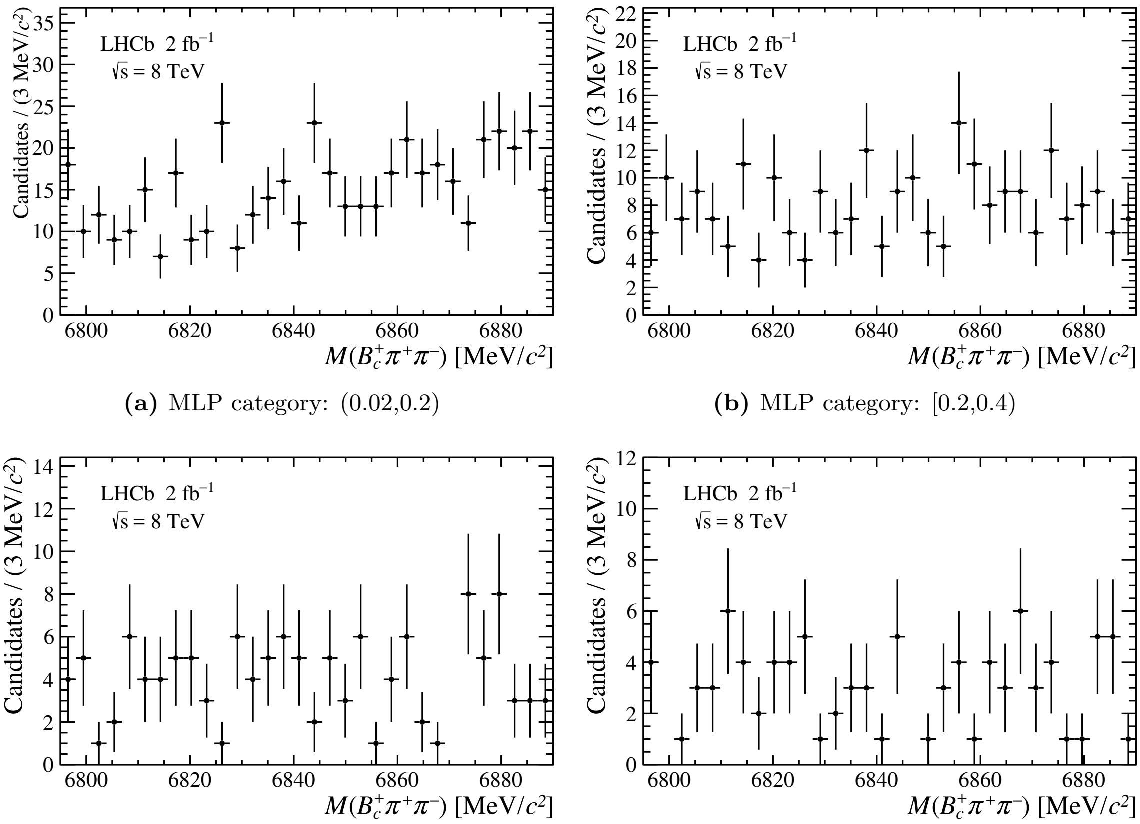

(a) MLP category: (0.02,0.2)

(b) MLP category: [0.2,0.4)

(c) MLP category: [0.4,0.6)

(d) MLP category: [0.6,1.0]

Figure 2. Mass distributions of the selected $B_c^+\pi^+\pi^-$ candidates in the range $[6795, 6890]\,\mathrm{MeV}/c^2$ for the four MLP categories.

in data and simulation are evaluated with the control decay mode $B_c^+ \to J/\psi\,\pi^+\pi^-\pi^+$, which has the same final state as the signal and a large yield, and are corrected by applying a scale factor. The obtained mass resolutions are $\sigma_{\mathrm{w}}(B_c(2S)^+) = 2.05 \pm 0.05\,\mathrm{MeV}/c^2$ and $\sigma_{\mathrm{w}}(B_c^*(2S)^+) = 3.17 \pm 0.03\,\mathrm{MeV}/c^2$. The $M(B_c^+\pi^+\pi^-)$ distributions are consistent with the background-only hypothesis, as determined by the scan described below.

4 Upper limits

As no significant $B_c^{(*)}(2S)^+$ signal is found, upper limits are set, for each $B_c^{(*)}(2S)^+$ mass hypothesis, on the ratio $\mathcal{R}$ of the $B_c^{(*)}(2S)^+$ production cross-section times the branching fraction of $B_c^{(*)}(2S)^+ \to B_c^{(*)+}\pi^+\pi^-$ to the production cross-section of the B_c^+ state. The ratio $\mathcal{R}$ is determined for $B_c^{(*)}(2S)^+$ and B_c^+ candidates in the kinematic ranges $p_{\mathrm{T}} \in [0, 20]\,\mathrm{GeV}/c$ and rapidity $y \in [2.0, 4.5]$, and is expressed as

$$\begin{aligned}\mathcal{R} &= \frac{\sigma_{B_c^{(*)}(2S)^+}}{\sigma_{B_c^+}} \cdot \mathcal{B}(B_c^{(*)}(2S)^+ \to B_c^{(*)+}\pi^+\pi^-) \\ &= \frac{N_{B_c^{(*)}(2S)^+}}{N_{B_c^+}} \cdot \frac{\varepsilon_{B_c^+}}{\varepsilon_{B_c^{(*)}(2S)^+}},\end{aligned} \tag{4.1}$$

JHEP01(2018)138

where σ is the production cross-section, N the yield, and ε the efficiency of reconstructing and selecting the B_c^+ or $B_c^{(*)}(2S)^+$ candidates in the required p_T and y regions. In the case $\Delta M = 0$, the reconstructed $B_c(2S)^+$ and $B_c^*(2S)^+$ states fully overlap, and the ratio $\mathcal{R}$ corresponds to the sum of the $\mathcal{R}$ values of the $B_c(2S)^+$ and $B_c^*(2S)^+$ states. The upper limits are calculated using the $\mathrm{CL_s}$ method [36], in which the upper limit for each mass hypothesis is obtained from the $\mathrm{CL_s}$ value calculated as a function of the ratio $\mathcal{R}$. The test statistic is the ratio of the likelihoods of the signal-plus-background hypothesis and the background-only hypothesis, defined as

$$\mathcal{Q}(N_\mathrm{obs}; N_S, N_B) = \frac{\mathcal{L}(N_\mathrm{obs}; N_S + N_B)}{\mathcal{L}(N_\mathrm{obs}; N_B)}, \tag{4.2}$$

where N_obs is the number of observed candidates, N_B is the expected background yield, and N_S is the expected signal yield. For a given value of the ratio $\mathcal{R}$, N_S is determined as

$$N_S = \mathcal{R} \cdot N_{B_c^+} \cdot \frac{\varepsilon_{B_c^{(*)}(2S)^+}}{\varepsilon_{B_c^+}}. \tag{4.3}$$

The likelihood $\mathcal{L}$ is defined as

$$\mathcal{L}(n; x) = \frac{e^{-x}}{n!} x^n. \tag{4.4}$$

The total statistical test value $\mathcal{Q}_\mathrm{tot}$ is the product of that for each of the four MLP categories. The $\mathrm{CL_s}$ value is the ratio of $\mathrm{CL_{s+b}}$ to $\mathrm{CL_b}$, where $\mathrm{CL_{s+b}}$ is the probability to find a $\mathcal{Q}_\mathrm{tot}$ value smaller than the $\mathcal{Q}_\mathrm{tot}$ value found in the data sample under the signal-plus-background hypothesis, and $\mathrm{CL_b}$ is equivalent probability under the background-only hypothesis. The $\mathrm{CL_{s+b}}$ and $\mathrm{CL_b}$ values are obtained from pseudoexperiments, in which the input variables are varied within their statistical and systematic uncertainties. The $B_c(2S)^+$ state is searched for by scanning the mass region $M(B_c^+\pi^+\pi^-) \in [6830, 6890]\,\mathrm{MeV}/c^2$, which is motivated by theoretical predictions [1–11]. The value of ΔM is successively fixed to 0, 15, 25 and 35 MeV/c^2. The search windows are within $\pm 1.4\sigma_\mathrm{w}(B_c^{(*)}(2S)^+)$ of the $B_c^{(*)}(2S)^+$ mass hypotheses. This choice of the search window gives the best sensitivity according to ref. [37].

The selection efficiencies $\varepsilon_{B_c^+}$ and $\varepsilon_{B_c^{(*)}(2S)^+}$ are estimated using simulation. The track reconstruction efficiency is studied in a data control sample of $J/\psi \to \mu^+\mu^-$ decays using a tag-and-probe technique [38], in which one of the muons is fully reconstructed as the tag track, and the other muon, the probe track, is reconstructed using only information from the TT detector and the muon stations. The track reconstruction efficiency is the fraction of J/ψ candidates whose probe tracks match fully reconstructed tracks. The particle-identification (PID) efficiency of the two opposite-charge pions is determined with a data-driven method, using a π^+ sample from D^*-tagged $D^0 \to K^-\pi^+$ decays. The total efficiency $\varepsilon_{B_c^+}$ is determined to be 0.0931 ± 0.0005, where the uncertainty is the statistical uncertainty of the simulated sample. The $B_c^{(*)}(2S)^+$ efficiencies obtained from the default simulation, where $M(B_c(2S)^+) = 6858\,\mathrm{MeV}/c^2$ and $M(B_c^*(2S)^+) = 6890\,\mathrm{MeV}/c^2$, are summarised in table 1. The variation of the efficiencies with respect to $M(B_c(2S)^+)$ and $M(B_c^*(2S)^+)$, assumed to be linear, is studied using the data simulated with different

MLP category	$(0.02, 0.2)$	$[0.2, 0.4)$	$[0.4, 0.6)$	$[0.6, 1.0]$
		Efficiencies in %		
$B_c(2S)^+$	0.148 ± 0.006	0.140 ± 0.006	0.130 ± 0.006	0.256 ± 0.008
$B_c^*(2S)^+$	0.118 ± 0.003	0.140 ± 0.004	0.144 ± 0.004	0.288 ± 0.005

Table 1. Efficiencies for the $B_c^{(*)}(2S)^+$ states in the regions $p_{\mathrm{T}} \in [0, 20]\,\mathrm{GeV}/c$ and $y \in [2.0, 4.5]$ for each MLP category. The efficiencies obtained before applying the MLP classifier are 0.0091 ± 0.0002 and 0.0086 ± 0.0001 for $B_c(2S)^+$ and $B_c^*(2S)^+$, respectively. The uncertainties are statistical only, and are due to the limited size of the simulated sample.

JHEP01(2018)138

mass settings. This variation is considered when searching for the $B_c^{(*)}(2S)^+$ states at other masses. The expected background yield in each of the $B_c^{(*)}(2S)^+$ signal regions, N_B, is estimated via extrapolation from the $M(B_c^+\pi^+\pi^-)$ sidebands for each MLP category. The background is modelled by an empirical threshold function as shown in figure 3, where the threshold is taken to be $M(B_c^+) + M(\pi^+) + M(\pi^-) = 6555\,\mathrm{MeV}/c^2$. The other parameters are fixed according to the $M(B_c^+\pi^+\pi^-)$ distribution of the same-sign sample, which is constructed with $B_c^+\pi^+\pi^+$ or $B_c^+\pi^-\pi^-$ combinations.

The sources of systematic uncertainties that affect the upper limit calculation are studied and summarised in table 2. The systematic uncertainty on $N_{B_c^+}$ comes from the potentially imperfect modelling of the signal, and has been studied using pseudoexperiments. The uncertainty on $\varepsilon_{B_c^+}$ is due to the limited size of the simulated sample. The uncertainty on N_B comes both from differences between the combinatorial backgrounds in the opposite-sign and the same-sign data samples and from the potential mismodelling of the background. The former is studied by performing a large set of pseudoexperiments, in which the samples are generated by randomly taking candidates from the data sample, while the candidates in $M(B_c^+\pi^+\pi^-) \in [6785, 6900]\,\mathrm{MeV}/c^2$ are taken from the same-sign sample. The $M(B_c^+\pi^+\pi^-)$ distributions of the pseudosamples are fit using the same function as in the nominal background modelling. The difference between the mean value of N_B obtained from the pseudoexperiments and the nominal value is taken as the systematic uncertainty. The potential mismodelling of the background is estimated by using the Bukin function [39] as an alternative model and the differences to the nominal results are taken as systematic uncertainties. The uncertainties on $\varepsilon_{B_c^{(*)}(2S)^+}$ are dominated by the uncertainty due to the finite size of the simulated samples, but also include the systematic uncertainties on the PID and track reconstruction efficiency calibration, which come from the limited size and the binning scheme of the calibration samples. The variations of efficiency with respect to $M(B_c(2S)^+)$ and $M(B_c^*(2S)^+)$ are fitted with linear functions, and the uncertainties of such fits are taken as systematic uncertainties.

No evidence of the $B_c^{(*)}(2S)^+$ signal is observed. The measurement is consistent with the background-only hypothesis for all mass assumptions. The upper limits at 90% and 95% confidence levels (CL) on the ratio $\mathcal{R}$, as functions of the $B_c^{(*)}(2S)^+$ mass states, are shown in figure 4. All the upper limits at 95% CL on the ratio $\mathcal{R}$ are contained

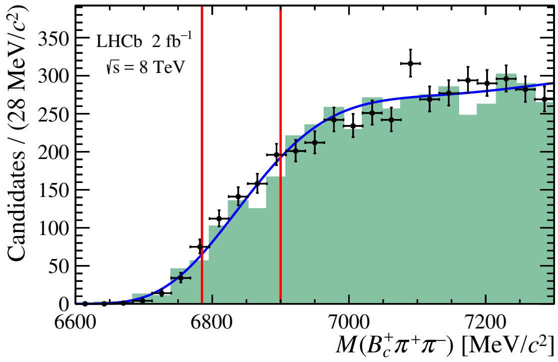

(a) MLP category: (0.02,0.2)

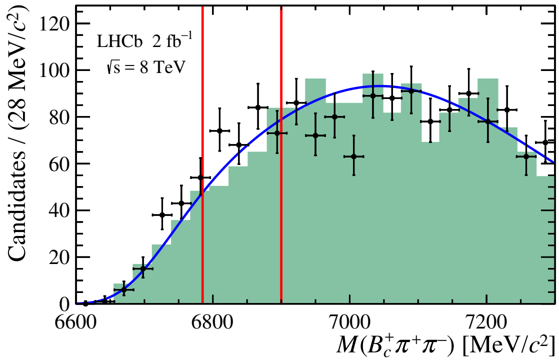

(b) MLP category: [0.2,0.4)

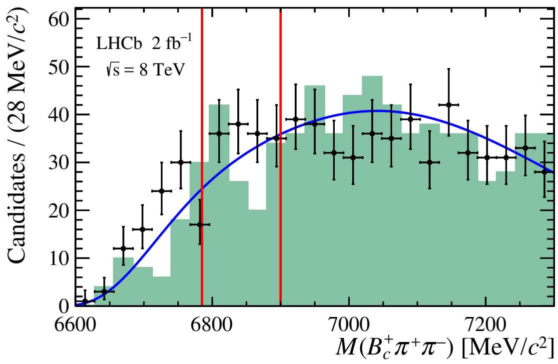

(c) MLP category: [0.4,0.6)

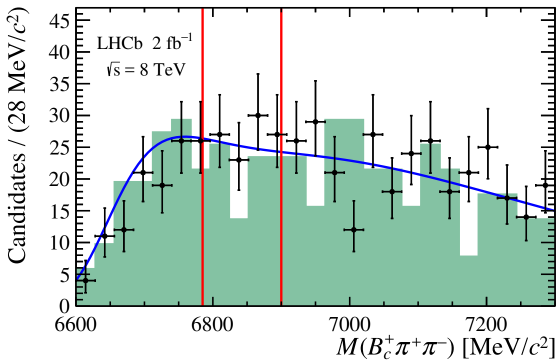

(d) MLP category: [0.6,1.0]

Figure 3. The $M(B_c^+\pi^+\pi^-)$ distributions in the same-sign (darkgreen shaded areas) and data (points with error bars) samples in the range $[6600, 7300]\,\text{MeV}/c^2$ with the background model (blue solid line) overlaid, for the four MLP categories. The areas between the two vertical red lines are the signal regions.

MLP category	$(0.02, 0.2)$	$[0.2, 0.4)$	$[0.4, 0.6)$	$[0.6, 1.0]$
$N_{B_c^+}$	1.0%			
$\varepsilon_{B_c^+}$	0.5%			
N_B	4.2%	9.0%	15.0%	6.9%
$B_c(2S)^+ \to B_c^+\pi^+\pi^-$				
$\varepsilon_{B_c(2S)^+}$	4.6%	4.7%	4.9%	3.6%
Efficiency variation *vs.* $M(B_c(2S)^+)$	0.6%	1.3%	1.8%	2.7%
$B_c^*(2S)^+ \to B_c^{*+}\pi^+\pi^-$				
$\varepsilon_{B_c^*(2S)^+}$	3.5%	3.3%	3.3%	2.7%
Efficiency variation *vs.* $M(B_c^*(2S)^+)$	1.0%	1.8%	2.5%	4.3%

Table 2. Summary of the systematic uncertainties entering the upper limit calculation for the four MLP categories.

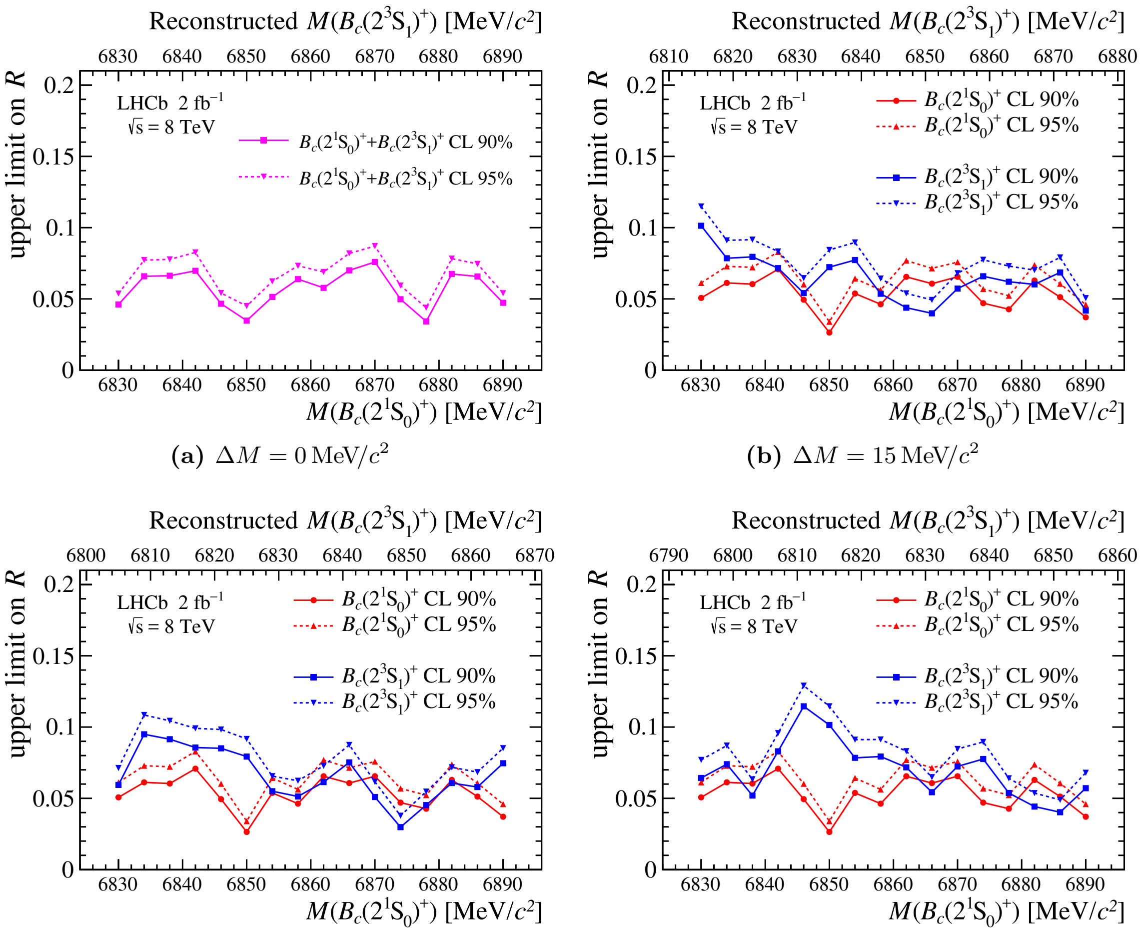

(a) $\Delta M = 0\,\mathrm{MeV}/c^2$ **(b)** $\Delta M = 15\,\mathrm{MeV}/c^2$

(c) $\Delta M = 25\,\mathrm{MeV}/c^2$ **(d)** $\Delta M = 35\,\mathrm{MeV}/c^2$

Figure 4. The upper limits on the ratio $\mathcal{R}(B_c^{(*)}(2S)^+)$ at 95% and 90% confidence levels under different mass splitting ΔM hypotheses.

between 0.02 and 0.14. Theoretical models predict that the ratio $\mathcal{R}$ has no significant dependence on y and p_{T} of the B_c^+ mesons [19], allowing comparison with the ATLAS result [18]. The most probable interpretation of the ATLAS measurement is that it is either the $B_c^*(2S)^+$ state or a sum of $B_c(2S)^+$ and $B_c^*(2S)^+$ signals under the $\Delta M \sim 0$ scenario. For both interpretations of the ATLAS measurement, the comparison of the ratio $\mathcal{R}$ between the LHCb upper limits in the vicinity of the peak claimed by ATLAS at $M(B_c^{(*)}(2S)^+) = 6842\ \mathrm{MeV}/c^2$ and the ratios determined by ATLAS are given in table 3. The LHCb and ATLAS results are compatible only in case of very large (unpublished) relative efficiency of reconstructing the $B_c^{(*)}(2S)^+$ candidates with respect to the B_c^+ signals for the ATLAS measurement.

	$\sqrt{s} = 7\,\text{TeV}$	$\sqrt{s} = 8\,\text{TeV}$
ATLAS	$(0.22 \pm 0.08\,(\text{stat}))/\varepsilon_7$	$(0.15 \pm 0.06\,(\text{stat}))/\varepsilon_8$
LHCb	–	$< [0.04, 0.09]$

Table 3. Comparison of the $\mathcal{R}$ value between the LHCb upper limits at 95% CL and the ATLAS measurement [18], where $0 < \varepsilon_{7,8} \leq 1$ are the relative efficiencies of reconstructing the $B_c^{(*)}(2S)^+$ candidates with respect to the B_c^+ signals for the 7 and 8 TeV data, respectively.

5 Summary

In summary, a search for the $B_c(2S)^+$ and $B_c^*(2S)^+$ states is performed at LHCb with a data sample of pp collisions, corresponding to an integrated luminosity of $2\,\text{fb}^{-1}$, recorded at a centre-of-mass energy of 8 TeV. No significant signal is found. Upper limits on the $B_c(2S)^+$ and $B_c^*(2S)^+$ production cross-sections times the branching fraction of $B_c^{(*)}(2S)^+ \to B_c^{(*)+}\pi^+\pi^-$ relative to the B_c^+ cross-section, are given as a function of the $B_c(2S)^+$ and $B_c^*(2S)^+$ masses.

Acknowledgments

We thank Chao-Hsi Chang and Xing-Gang Wu for frequent and interesting discussions on the production of the B_c mesons. We express our gratitude to our colleagues in the CERN accelerator departments for the excellent performance of the LHC. We thank the technical and administrative staff at the LHCb institutes. We acknowledge support from CERN and from the national agencies: CAPES, CNPq, FAPERJ and FINEP (Brazil); MOST and NSFC (China); CNRS/IN2P3 (France); BMBF, DFG and MPG (Germany); INFN (Italy); NWO (The Netherlands); MNiSW and NCN (Poland); MEN/IFA (Romania); MinES and FASO (Russia); MinECo (Spain); SNSF and SER (Switzerland); NASU (Ukraine); STFC (United Kingdom); NSF (U.S.A.). We acknowledge the computing resources that are provided by CERN, IN2P3 (France), KIT and DESY (Germany), INFN (Italy), SURF (The Netherlands), PIC (Spain), GridPP (United Kingdom), RRCKI and Yandex LLC (Russia), CSCS (Switzerland), IFIN-HH (Romania), CBPF (Brazil), PL-GRID (Poland) and OSC (U.S.A.). We are indebted to the communities behind the multiple open-source software packages on which we depend. Individual groups or members have received support from AvH Foundation (Germany), EPLANET, Marie Skłodowska-Curie Actions and ERC (European Union), ANR, Labex P2IO, ENIGMASS and OCEVU, and Région Auvergne-Rhône-Alpes (France), RFBR and Yandex LLC (Russia), GVA, XuntaGal and GENCAT (Spain), Herchel Smith Fund, the Royal Society, the English-Speaking Union and the Leverhulme Trust (United Kingdom).

JHEP01(2018)138

References

[1] S.S. Gershtein, V.V. Kiselev, A.K. Likhoded, S.R. Slabospitsky and A.V. Tkabladze, *Production Cross-sections and Spectroscopy of B_c Mesons*, *Sov. J. Nucl. Phys.* **48** (1988) 327 [INSPIRE].

[2] Y.-Q. Chen and Y.-P. Kuang, *Improved QCD motivated heavy quark potentials with explicit $\Lambda_{\overline{\rm MS}}$ dependence*, *Phys. Rev.* **D 46** (1992) 1165 [*Erratum ibid.* **D 47** (1993) 350] [INSPIRE].

[3] E.J. Eichten and C. Quigg, *Mesons with beauty and charm: Spectroscopy*, *Phys. Rev.* **D 49** (1994) 5845 [hep-ph/9402210] [INSPIRE].

[4] V.V. Kiselev, A.K. Likhoded and A.V. Tkabladze, *B_c spectroscopy*, *Phys. Rev.* **D 51** (1995) 3613 [hep-ph/9406339] [INSPIRE].

[5] S.N. Gupta and J.M. Johnson, *B_c spectroscopy in a quantum chromodynamic potential model*, *Phys. Rev.* **D 53** (1996) 312 [hep-ph/9511267] [INSPIRE].

[6] L.P. Fulcher, *Phenomenological predictions of the properties of the B_c system*, *Phys. Rev.* **D 60** (1999) 074006 [hep-ph/9806444] [INSPIRE].

[7] D. Ebert, R.N. Faustov and V.O. Galkin, *Properties of heavy quarkonia and B_c mesons in the relativistic quark model*, *Phys. Rev.* **D 67** (2003) 014027 [hep-ph/0210381] [INSPIRE].

[8] S. Godfrey, *Spectroscopy of B_c mesons in the relativized quark model*, *Phys. Rev.* **D 70** (2004) 054017 [hep-ph/0406228] [INSPIRE].

[9] K.-W. Wei and X.-H. Guo, *Mass spectra of doubly heavy mesons in Regge phenomenology*, *Phys. Rev.* **D 81** (2010) 076005 [INSPIRE].

[10] A.K. Rai and P.C. Vinodkumar, *Properties of B_c meson*, *Pramana* **66** (2006) 953 [hep-ph/0606194] [INSPIRE].

[11] A. Abd El-Hady, J.R. Spence and J.P. Vary, *Radiative decays of B_c mesons in a Bethe-Salpeter model*, *Phys. Rev.* **D 71** (2005) 034006 [hep-ph/0603139] [INSPIRE].

[12] A.V. Berezhnoy, V.V. Kiselev, A.K. Likhoded and A.I. Onishchenko, *B_c meson at LHC*, *Phys. Atom. Nucl.* **60** (1997) 1729 [hep-ph/9703341] [INSPIRE].

[13] I.P. Gouz, V.V. Kiselev, A.K. Likhoded, V.I. Romanovsky and O.P. Yushchenko, *Prospects for the B_c studies at LHCb*, *Phys. Atom. Nucl.* **67** (2004) 1559 [hep-ph/0211432] [INSPIRE].

[14] K. Cheung and T.C. Yuan, *Hadronic production of S wave and P wave charmed beauty mesons via heavy quark fragmentation*, *Phys. Rev.* **D 53** (1996) 1232 [hep-ph/9502250] [INSPIRE].

[15] C.T.H. Davies, K. Hornbostel, G.P. Lepage, A.J. Lidsey, J. Shigemitsu and J.H. Sloan, *B_c spectroscopy from lattice QCD*, *Phys. Lett.* **B 382** (1996) 131 [hep-lat/9602020] [INSPIRE].

[16] CDF collaboration, F. Abe et al., *Observation of the B_c meson in $p\bar{p}$ collisions at $\sqrt{s} = 1.8$ TeV*, *Phys. Rev. Lett.* **81** (1998) 2432 [hep-ex/9805034] [INSPIRE].

[17] CDF collaboration, F. Abe et al., *Observation of B_c mesons in $p\bar{p}$ collisions at $\sqrt{s} = 1.8$ TeV*, *Phys. Rev.* **D 58** (1998) 112004 [hep-ex/9804014] [INSPIRE].

[18] ATLAS collaboration, *Observation of an Excited $B_c^{\pm}$ Meson State with the ATLAS Detector*, *Phys. Rev. Lett.* **113** (2014) 212004 [arXiv:1407.1032] [INSPIRE].

[19] C.-H. Chang, J.-X. Wang and X.-G. Wu, *BCVEGPY2.0: A Upgrade version of the generator BCVEGPY with an addendum about hadroproduction of the P-wave B_c states*, *Comput. Phys. Commun.* **174** (2006) 241 [hep-ph/0504017] [INSPIRE].

[20] Y.-N. Gao, J. He, P. Robbe, M.-H. Schune and Z.-W. Yang, *Experimental prospects of the B_c studies of the LHCb experiment*, *Chin. Phys. Lett.* **27** (2010) 061302 [INSPIRE].

[21] A. Berezhnoy and A. Likhoded, *The observation possibility of B_c excitations at LHC*, PoS(QFTHEP 2013)051 [arXiv:1307.5993] [INSPIRE].

[22] LHCb collaboration, *The LHCb Detector at the LHC*, 2008 *JINST* **3** S08005 [INSPIRE].

[23] LHCb collaboration, *LHCb Detector Performance*, *Int. J. Mod. Phys.* **A 30** (2015) 1530022 [arXiv:1412.6352] [INSPIRE].

[24] T. Sjöstrand, S. Mrenna and P.Z. Skands, *PYTHIA 6.4 Physics and Manual*, *JHEP* **05** (2006) 026 [hep-ph/0603175] [INSPIRE].

[25] I. Belyaev et al., *Handling of the generation of primary events in Gauss, the LHCb simulation framework*, *J. Phys. Conf. Ser.* **331** (2011) 032047 [INSPIRE].

[26] D.J. Lange, *The EvtGen particle decay simulation package*, *Nucl. Instrum. Meth.* **A 462** (2001) 152 [INSPIRE].

[27] P. Golonka and Z. Was, *PHOTOS Monte Carlo: A precision tool for QED corrections in Z and W decays*, *Eur. Phys. J.* **C 45** (2006) 97 [hep-ph/0506026] [INSPIRE].

[28] GEANT4 collaboration, J. Allison et al., *Geant4 developments and applications*, *IEEE Trans. Nucl. Sci.* **53** (2006) 270.

[29] M. Clemencic et al., *The LHCb simulation application, Gauss: Design, evolution and experience*, *J. Phys. Conf. Ser.* **331** (2011) 032023 [INSPIRE].

[30] L. Breiman, J.H. Friedman, R.A. Olshen and C.J. Stone, *Classification and regression trees*, Wadsworth international group, Belmont, California, U.S.A. (1984).

[31] Y. Freund and R.E. Schapire, *A decision-theoretic generalization of on-line learning and an application to boosting*, *J. Comput. Syst. Sci.* **55** (1997) 119.

[32] PARTICLE DATA GROUP collaboration, K.A. Olive et al., *Review of Particle Physics*, *Chin. Phys.* **C 38** (2014) 090001 [INSPIRE].

[33] PARTICLE DATA GROUP collaboration, C. Patrignani et al., *Review of Particle Physics*, *Chin. Phys.* **C 40** (2016) 100001 [INSPIRE].

[34] LHCb collaboration, *Measurements of B_c^+ production and mass with the $B_c^+ \to J/\psi\pi^+$ decay*, *Phys. Rev. Lett.* **109** (2012) 232001 [LHCb-PAPER-2012-028, CERN-PH-EP-2012-275] [arXiv:1209.5634] [INSPIRE].

[35] A. Hocker et al., *TMVA: Toolkit for Multivariate Data Analysis*, PoS(ACAT)040 [physics/0703039] [INSPIRE].

[36] A.L. Read, *Presentation of search results: The CL_s technique*, *J. Phys.* **G 28** (2002) 2693 [INSPIRE].

[37] V. Tisserand, *Optimisation du détecteur ATLAS pour la recherche du boson de Higgs se désintegrant en deux photons au LHC*, Ph.D. Thesis, LAL, Orsay (1997).

[38] LHCb collaboration, *Measurement of the track reconstruction efficiency at LHCb*, 2015 *JINST* **10** P02007 [arXiv:1408.1251] [INSPIRE].

[39] Z.K. Silagadze, *Finding two-dimensional peaks*, *Phys. Part. Nucl. Lett.* **4** (2007) 73 [physics/0402085] [INSPIRE].

JHEP01(2018)138

The LHCb collaboration

R. Aaij[40], B. Adeva[39], M. Adinolfi[48], Z. Ajaltouni[5], S. Akar[59], J. Albrecht[10], F. Alessio[40], M. Alexander[53], A. Alfonso Albero[38], S. Ali[43], G. Alkhazov[31], P. Alvarez Cartelle[55], A.A. Alves Jr[59], S. Amato[2], S. Amerio[23], Y. Amhis[7], L. An[3], L. Anderlini[18], G. Andreassi[41], M. Andreotti[17,g], J.E. Andrews[60], R.B. Appleby[56], F. Archilli[43], P. d'Argent[12], J. Arnau Romeu[6], A. Artamonov[37], M. Artuso[61], E. Aslanides[6], M. Atzeni[42], G. Auriemma[26], M. Baalouch[5], I. Babuschkin[56], S. Bachmann[12], J.J. Back[50], A. Badalov[38,m], C. Baesso[62], S. Baker[55], V. Balagura[7,b], W. Baldini[17], A. Baranov[35], R.J. Barlow[56], C. Barschel[40], S. Barsuk[7], W. Barter[56], F. Baryshnikov[32], V. Batozskaya[29], V. Battista[41], A. Bay[41], L. Beaucourt[4], J. Beddow[53], F. Bedeschi[24], I. Bediaga[1], A. Beiter[61], L.J. Bel[43], N. Beliy[63], V. Bellee[41], N. Belloli[21,i], K. Belous[37], I. Belyaev[32,40], E. Ben-Haim[8], G. Bencivenni[19], S. Benson[43], S. Beranek[9], A. Berezhnoy[33], R. Bernet[42], D. Berninghoff[12], E. Bertholet[8], A. Bertolin[23], C. Betancourt[42], F. Betti[15], M.O. Bettler[40], M. van Beuzekom[43], Ia. Bezshyiko[42], S. Bifani[47], P. Billoir[8], A. Birnkraut[10], A. Bizzeti[18,u], M. Bjørn[57], T. Blake[50], F. Blanc[41], S. Blusk[61], V. Bocci[26], T. Boettcher[58], A. Bondar[36,w], N. Bondar[31], I. Bordyuzhin[32], S. Borghi[56,40], M. Borisyak[35], M. Borsato[39], F. Bossu[7], M. Boubdir[9], T.J.V. Bowcock[54], E. Bowen[42], C. Bozzi[17,40], S. Braun[12], J. Brodzicka[27], D. Brundu[16], E. Buchanan[48], C. Burr[56], A. Bursche[16,f], J. Buytaert[40], W. Byczynski[40], S. Cadeddu[16], H. Cai[64], R. Calabrese[17,g], R. Calladine[47], M. Calvi[21,i], M. Calvo Gomez[38,m], A. Camboni[38,m], P. Campana[19], D.H. Campora Perez[40], L. Capriotti[56], A. Carbone[15,e], G. Carboni[25,j], R. Cardinale[20,h], A. Cardini[16], P. Carniti[21,i], L. Carson[52], K. Carvalho Akiba[2], G. Casse[54], L. Cassina[21], M. Cattaneo[40], G. Cavallero[20,40,h], R. Cenci[24,t], D. Chamont[7], M.G. Chapman[48], M. Charles[8], Ph. Charpentier[40], G. Chatzikonstantinidis[47], M. Chefdeville[4], S. Chen[16], S.F. Cheung[57], S.-G. Chitic[40], V. Chobanova[39], M. Chrzaszcz[42], A. Chubykin[31], P. Ciambrone[19], X. Cid Vidal[39], G. Ciezarek[40], P.E.L. Clarke[52], M. Clemencic[40], H.V. Cliff[49], J. Closier[40], V. Coco[40], J. Cogan[6], E. Cogneras[5], V. Cogoni[16,f], L. Cojocariu[30], P. Collins[40], T. Colombo[40], A. Comerma-Montells[12], A. Contu[16], G. Coombs[40], S. Coquereau[38], G. Corti[40], M. Corvo[17,g], C.M. Costa Sobral[50], B. Couturier[40], G.A. Cowan[52], D.C. Craik[58], A. Crocombe[50], M. Cruz Torres[1], R. Currie[52], C. D'Ambrosio[40], F. Da Cunha Marinho[2], C.L. Da Silva[72], E. Dall'Occo[43], J. Dalseno[48], A. Davis[3], O. De Aguiar Francisco[40], K. De Bruyn[40], S. De Capua[56], M. De Cian[12], J.M. De Miranda[1], L. De Paula[2], M. De Serio[14,d], P. De Simone[19], C.T. Dean[53], D. Decamp[4], L. Del Buono[8], H.-P. Dembinski[11], M. Demmer[10], A. Dendek[28], D. Derkach[35], O. Deschamps[5], F. Dettori[54], B. Dey[65], A. Di Canto[40], P. Di Nezza[19], H. Dijkstra[40], F. Dordei[40], M. Dorigo[40], A. Dosil Suárez[39], L. Douglas[53], A. Dovbnya[45], K. Dreimanis[54], L. Dufour[43], G. Dujany[8], P. Durante[40], J.M. Durham[72], D. Dutta[56], R. Dzhelyadin[37], M. Dziewiecki[12], A. Dziurda[40], A. Dzyuba[31], S. Easo[51], M. Ebert[52], U. Egede[55], V. Egorychev[32], S. Eidelman[36,w], S. Eisenhardt[52], U. Eitschberger[10], R. Ekelhof[10], L. Eklund[53], S. Ely[61], S. Esen[12], H.M. Evans[49], T. Evans[57], A. Falabella[15], N. Farley[47], S. Farry[54], D. Fazzini[21,i], L. Federici[25], D. Ferguson[52], G. Fernandez[38], P. Fernandez Declara[40], A. Fernandez Prieto[39], F. Ferrari[15], L. Ferreira Lopes[41], F. Ferreira Rodrigues[2], M. Ferro-Luzzi[40], S. Filippov[34], R.A. Fini[14], M. Fiorini[17,g], M. Firlej[28], C. Fitzpatrick[41], T. Fiutowski[28], F. Fleuret[7,b], M. Fontana[16,40], F. Fontanelli[20,h], R. Forty[40], V. Franco Lima[54], M. Frank[40], C. Frei[40], J. Fu[22,q], W. Funk[40], E. Furfaro[25,j], C. Färber[40], E. Gabriel[52], A. Gallas Torreira[39], D. Galli[15,e], S. Gallorini[23], S. Gambetta[52], M. Gandelman[2], P. Gandini[22], Y. Gao[3], L.M. Garcia Martin[70], J. García Pardiñas[39], J. Garra Tico[49], L. Garrido[38], P.J. Garsed[49], D. Gascon[38], C. Gaspar[40], L. Gavardi[10], G. Gazzoni[5], D. Gerick[12], E. Gersabeck[56], M. Gersabeck[56], T. Gershon[50], Ph. Ghez[4], S. Gianì[41], V. Gibson[49], O.G. Girard[41], L. Giubega[30], K. Gizdov[52], V.V. Gligorov[8], D. Golubkov[32], A. Golutvin[55],

JHEP01(2018)138

A. Gomes[1,a], I.V. Gorelov[33], C. Gotti[21,i], E. Govorkova[43], J.P. Grabowski[12], R. Graciani Diaz[38], L.A. Granado Cardoso[40], E. Graugés[38], E. Graverini[42], G. Graziani[18], A. Grecu[30], R. Greim[9], P. Griffith[16], L. Grillo[56], L. Gruber[40], B.R. Gruberg Cazon[57], O. Grünberg[67], E. Gushchin[34], Yu. Guz[37], T. Gys[40], C. Göbel[62], T. Hadavizadeh[57], C. Hadjivasiliou[5], G. Haefeli[41], C. Haen[40], S.C. Haines[49], B. Hamilton[60], X. Han[12], T.H. Hancock[57], S. Hansmann-Menzemer[12], N. Harnew[57], S.T. Harnew[48], C. Hasse[40], M. Hatch[40], J. He[63], M. Hecker[55], K. Heinicke[10], A. Heister[9], K. Hennessy[54], P. Henrard[5], L. Henry[70], E. van Herwijnen[40], M. Heß[67], A. Hicheur[2], D. Hill[57], P.H. Hopchev[41], W. Hu[65], W. Huang[63], Z.C. Huard[59], W. Hulsbergen[43], T. Humair[55], M. Hushchyn[35], D. Hutchcroft[54], P. Ibis[10], M. Idzik[28], P. Ilten[47], R. Jacobsson[40], J. Jalocha[57], E. Jans[43], A. Jawahery[60], F. Jiang[3], M. John[57], D. Johnson[40], C.R. Jones[49], C. Joram[40], B. Jost[40], N. Jurik[57], S. Kandybei[45], M. Karacson[40], J.M. Kariuki[48], S. Karodia[53], N. Kazeev[35], M. Kecke[12], F. Keizer[49], M. Kelsey[61], M. Kenzie[49], T. Ketel[44], E. Khairullin[35], B. Khanji[12], C. Khurewathanakul[41], T. Kirn[9], S. Klaver[19], K. Klimaszewski[29], T. Klimkovich[11], S. Koliiev[46], M. Kolpin[12], R. Kopecna[12], P. Koppenburg[43], A. Kosmyntseva[32], S. Kotriakhova[31], M. Kozeiha[5], L. Kravchuk[34], M. Kreps[50], F. Kress[55], P. Krokovny[36,w], W. Krzemien[29], W. Kucewicz[27,l], M. Kucharczyk[27], V. Kudryavtsev[36,w], A.K. Kuonen[41], T. Kvaratskheliya[32,40], D. Lacarrere[40], G. Lafferty[56], A. Lai[16], G. Lanfranchi[19], C. Langenbruch[9], T. Latham[50], C. Lazzeroni[47], R. Le Gac[6], A. Leflat[33,40], J. Lefrançois[7], R. Lefèvre[5], F. Lemaitre[40], E. Lemos Cid[39], O. Leroy[6], T. Lesiak[27], B. Leverington[12], P.-R. Li[63], T. Li[3], Y. Li[7], Z. Li[61], X. Liang[61], T. Likhomanenko[68], R. Lindner[40], F. Lionetto[42], V. Lisovskyi[7], X. Liu[3], D. Loh[50], A. Loi[16], I. Longstaff[53], J.H. Lopes[2], D. Lucchesi[23,o], M. Lucio Martinez[39], H. Luo[52], A. Lupato[23], E. Luppi[17,g], O. Lupton[40], A. Lusiani[24], X. Lyu[63], F. Machefert[7], F. Maciuc[30], V. Macko[41], P. Mackowiak[10], S. Maddrell-Mander[48], O. Maev[31,40], K. Maguire[56], D. Maisuzenko[31], M.W. Majewski[28], S. Malde[57], B. Malecki[27], A. Malinin[68], T. Maltsev[36,w], G. Manca[16,f], G. Mancinelli[6], D. Marangotto[22,q], J. Maratas[5,v], J.F. Marchand[4], U. Marconi[15], C. Marin Benito[38], M. Marinangeli[41], P. Marino[41], J. Marks[12], G. Martellotti[26], M. Martin[6], M. Martinelli[41], D. Martinez Santos[39], F. Martinez Vidal[70], A. Massafferri[1], R. Matev[40], A. Mathad[50], Z. Mathe[40], C. Matteuzzi[21], A. Mauri[42], E. Maurice[7,b], B. Maurin[41], A. Mazurov[47], M. McCann[55,40], A. McNab[56], R. McNulty[13], J.V. Mead[54], B. Meadows[59], C. Meaux[6], F. Meier[10], N. Meinert[67], D. Melnychuk[29], M. Merk[43], A. Merli[22,40,q], E. Michielin[23], D.A. Milanes[66], E. Millard[50], M.-N. Minard[4], L. Minzoni[17], D.S. Mitzel[12], A. Mogini[8], J. Molina Rodriguez[1], T. Mombächer[10], I.A. Monroy[66], S. Monteil[5], M. Morandin[23], M.J. Morello[24,t], O. Morgunova[68], J. Moron[28], A.B. Morris[52], R. Mountain[61], F. Muheim[52], M. Mulder[43], D. Müller[56], J. Müller[10], K. Müller[42], V. Müller[10], P. Naik[48], T. Nakada[41], R. Nandakumar[51], A. Nandi[57], I. Nasteva[2], M. Needham[52], N. Neri[22,40], S. Neubert[12], N. Neufeld[40], M. Neuner[12], T.D. Nguyen[41], C. Nguyen-Mau[41,n], S. Nieswand[9], R. Niet[10], N. Nikitin[33], T. Nikodem[12], A. Nogay[68], D.P. O'Hanlon[50], A. Oblakowska-Mucha[28], V. Obraztsov[37], S. Ogilvy[19], R. Oldeman[16,f], C.J.G. Onderwater[71], A. Ossowska[27], J.M. Otalora Goicochea[2], P. Owen[42], A. Oyanguren[70], P.R. Pais[41], A. Palano[14], M. Palutan[19,40], A. Papanestis[51], M. Pappagallo[52], L.L. Pappalardo[17,g], W. Parker[60], C. Parkes[56], G. Passaleva[18,40], A. Pastore[14,d], M. Patel[55], C. Patrignani[15,e], A. Pearce[40], A. Pellegrino[43], G. Penso[26], M. Pepe Altarelli[40], S. Perazzini[40], D. Pereima[32], P. Perret[5], L. Pescatore[41], K. Petridis[48], A. Petrolini[20,h], A. Petrov[68], M. Petruzzo[22,q], E. Picatoste Olloqui[38], B. Pietrzyk[4], G. Pietrzyk[41], M. Pikies[27], D. Pinci[26], F. Pisani[40], A. Pistone[20,h], A. Piucci[12], V. Placinta[30], S. Playfer[52], M. Plo Casasus[39], F. Polci[8], M. Poli Lener[19], A. Poluektov[50], I. Polyakov[61], E. Polycarpo[2], G.J. Pomery[48], S. Ponce[40], A. Popov[37], D. Popov[11,40], S. Poslavskii[37], C. Potterat[2], E. Price[48], J. Prisciandaro[39], C. Prouve[48], V. Pugatch[46], A. Puig Navarro[42], H. Pullen[57], G. Punzi[24,p], W. Qian[50], J. Qin[63], R. Quagliani[8], B. Quintana[5], B. Rachwal[28], J.H. Rademacker[48], M. Rama[24], M. Ramos Pernas[39],

JHEP01(2018)138

M.S. Rangel[2], I. Raniuk[45,†], F. Ratnikov[35], G. Raven[44], M. Ravonel Salzgeber[40], M. Reboud[4], F. Redi[41], S. Reichert[10], A.C. dos Reis[1], C. Remon Alepuz[70], V. Renaudin[7], S. Ricciardi[51], S. Richards[48], M. Rihl[40], K. Rinnert[54], P. Robbe[7], A. Robert[8], A.B. Rodrigues[41], E. Rodrigues[59], J.A. Rodriguez Lopez[66], A. Rogozhnikov[35], S. Roiser[40], A. Rollings[57], V. Romanovskiy[37], A. Romero Vidal[39,40], M. Rotondo[19], M.S. Rudolph[61], T. Ruf[40], P. Ruiz Valls[70], J. Ruiz Vidal[70], J.J. Saborido Silva[39], E. Sadykhov[32], N. Sagidova[31], B. Saitta[16,f], V. Salustino Guimaraes[62], C. Sanchez Mayordomo[70], B. Sanmartin Sedes[39], R. Santacesaria[26], C. Santamarina Rios[39], M. Santimaria[19], E. Santovetti[25,j], G. Sarpis[56], A. Sarti[19,k], C. Satriano[26,s], A. Satta[25], D.M. Saunders[48], D. Savrina[32,33], S. Schael[9], M. Schellenberg[10], M. Schiller[53], H. Schindler[40], M. Schmelling[11], T. Schmelzer[10], B. Schmidt[40], O. Schneider[41], A. Schopper[40], H.F. Schreiner[59], M. Schubiger[41], M.H. Schune[7], R. Schwemmer[40], B. Sciascia[19], A. Sciubba[26,k], A. Semennikov[32], E.S. Sepulveda[8], A. Sergi[47], N. Serra[42], J. Serrano[6], L. Sestini[23], P. Seyfert[40], M. Shapkin[37], I. Shapoval[45], Y. Shcheglov[31], T. Shears[54], L. Shekhtman[36,w], V. Shevchenko[68], B.G. Siddi[17], R. Silva Coutinho[42], L. Silva de Oliveira[2], G. Simi[23,o], S. Simone[14,d], M. Sirendi[49], N. Skidmore[48], T. Skwarnicki[61], I.T. Smith[52], J. Smith[49], M. Smith[55], l. Soares Lavra[1], M.D. Sokoloff[59], F.J.P. Soler[53], B. Souza De Paula[2], B. Spaan[10], P. Spradlin[53], S. Sridharan[40], F. Stagni[40], M. Stahl[12], S. Stahl[40], P. Stefko[41], S. Stefkova[55], O. Steinkamp[42], S. Stemmle[12], O. Stenyakin[37], M. Stepanova[31], H. Stevens[10], S. Stone[61], B. Storaci[42], S. Stracka[24,p], M.E. Stramaglia[41], M. Straticiuc[30], U. Straumann[42], J. Sun[3], L. Sun[64], K. Swientek[28], V. Syropoulos[44], T. Szumlak[28], M. Szymanski[63], S. T'Jampens[4], A. Tayduganov[6], T. Tekampe[10], G. Tellarini[17,g], F. Teubert[40], E. Thomas[40], J. van Tilburg[43], M.J. Tilley[55], V. Tisserand[5], M. Tobin[41], S. Tolk[49], L. Tomassetti[17,g], D. Tonelli[24], R. Tourinho Jadallah Aoude[1], E. Tournefier[4], M. Traill[53], M.T. Tran[41], M. Tresch[42], A. Trisovic[49], A. Tsaregorodtsev[6], P. Tsopelas[43], A. Tully[49], N. Tuning[43,40], A. Ukleja[29], A. Usachov[7], A. Ustyuzhanin[35], U. Uwer[12], C. Vacca[16,f], A. Vagner[69], V. Vagnoni[15,40], A. Valassi[40], S. Valat[40], G. Valenti[15], R. Vazquez Gomez[40], P. Vazquez Regueiro[39], S. Vecchi[17], M. van Veghel[43], J.J. Velthuis[48], M. Veltri[18,r], G. Veneziano[57], A. Venkateswaran[61], T.A. Verlage[9], M. Vernet[5], M. Vesterinen[57], J.V. Viana Barbosa[40], D. Vieira[63], M. Vieites Diaz[39], H. Viemann[67], X. Vilasis-Cardona[38,m], M. Vitti[49], V. Volkov[33], A. Vollhardt[42], B. Voneki[40], A. Vorobyev[31], V. Vorobyev[36,w], C. Voß[9], J.A. de Vries[43], C. Vázquez Sierra[43], R. Waldi[67], J. Walsh[24], J. Wang[61], Y. Wang[65], D.R. Ward[49], H.M. Wark[54], N.K. Watson[47], D. Websdale[55], A. Weiden[42], C. Weisser[58], M. Whitehead[40], J. Wicht[50], G. Wilkinson[57], M. Wilkinson[61], M. Williams[56], M. Williams[58], T. Williams[47], F.F. Wilson[51,40], J. Wimberley[60], M. Winn[7], J. Wishahi[10], W. Wislicki[29], M. Witek[27], G. Wormser[7], S.A. Wotton[49], K. Wyllie[40], Y. Xie[65], M. Xu[65], Q. Xu[63], Z. Xu[3], Z. Xu[4], Z. Yang[3], Z. Yang[60], Y. Yao[61], H. Yin[65], J. Yu[65], X. Yuan[61], O. Yushchenko[37], K.A. Zarebski[47], M. Zavertyaev[11,c], L. Zhang[3], Y. Zhang[7], A. Zhelezov[12], Y. Zheng[63], X. Zhu[3], V. Zhukov[9,33], J.B. Zonneveld[52], S. Zucchelli[15]

[1] *Centro Brasileiro de Pesquisas Físicas (CBPF), Rio de Janeiro, Brazil*
[2] *Universidade Federal do Rio de Janeiro (UFRJ), Rio de Janeiro, Brazil*
[3] *Center for High Energy Physics, Tsinghua University, Beijing, China*
[4] *Univ. Grenoble Alpes, Univ. Savoie Mont Blanc, CNRS, IN2P3-LAPP, Annecy, France*
[5] *Clermont Université, Université Blaise Pascal, CNRS/IN2P3, LPC, Clermont-Ferrand, France*
[6] *Aix Marseille Univ, CNRS/IN2P3, CPPM, Marseille, France*
[7] *LAL, Univ. Paris-Sud, CNRS/IN2P3, Université Paris-Saclay, Orsay, France*
[8] *LPNHE, Université Pierre et Marie Curie, Université Paris Diderot, CNRS/IN2P3, Paris, France*
[9] *I. Physikalisches Institut, RWTH Aachen University, Aachen, Germany*
[10] *Fakultät Physik, Technische Universität Dortmund, Dortmund, Germany*
[11] *Max-Planck-Institut für Kernphysik (MPIK), Heidelberg, Germany*

JHEP01(2018)138

[12] *Physikalisches Institut, Ruprecht-Karls-Universität Heidelberg, Heidelberg, Germany*
[13] *School of Physics, University College Dublin, Dublin, Ireland*
[14] *Sezione INFN di Bari, Bari, Italy*
[15] *Sezione INFN di Bologna, Bologna, Italy*
[16] *Sezione INFN di Cagliari, Cagliari, Italy*
[17] *Universita e INFN, Ferrara, Ferrara, Italy*
[18] *Sezione INFN di Firenze, Firenze, Italy*
[19] *Laboratori Nazionali dell'INFN di Frascati, Frascati, Italy*
[20] *Sezione INFN di Genova, Genova, Italy*
[21] *Sezione INFN di Milano Bicocca, Milano, Italy*
[22] *Sezione di Milano, Milano, Italy*
[23] *Sezione INFN di Padova, Padova, Italy*
[24] *Sezione INFN di Pisa, Pisa, Italy*
[25] *Sezione INFN di Roma Tor Vergata, Roma, Italy*
[26] *Sezione INFN di Roma La Sapienza, Roma, Italy*
[27] *Henryk Niewodniczanski Institute of Nuclear Physics Polish Academy of Sciences, Kraków, Poland*
[28] *AGH - University of Science and Technology, Faculty of Physics and Applied Computer Science, Kraków, Poland*
[29] *National Center for Nuclear Research (NCBJ), Warsaw, Poland*
[30] *Horia Hulubei National Institute of Physics and Nuclear Engineering, Bucharest-Magurele, Romania*
[31] *Petersburg Nuclear Physics Institute (PNPI), Gatchina, Russia*
[32] *Institute of Theoretical and Experimental Physics (ITEP), Moscow, Russia*
[33] *Institute of Nuclear Physics, Moscow State University (SINP MSU), Moscow, Russia*
[34] *Institute for Nuclear Research of the Russian Academy of Sciences (INR RAN), Moscow, Russia*
[35] *Yandex School of Data Analysis, Moscow, Russia*
[36] *Budker Institute of Nuclear Physics (SB RAS), Novosibirsk, Russia*
[37] *Institute for High Energy Physics (IHEP), Protvino, Russia*
[38] *ICCUB, Universitat de Barcelona, Barcelona, Spain*
[39] *Instituto Galego de Física de Altas Enerxías (IGFAE), Universidade de Santiago de Compostela, Santiago de Compostela, Spain*
[40] *European Organization for Nuclear Research (CERN), Geneva, Switzerland*
[41] *Institute of Physics, Ecole Polytechnique Fédérale de Lausanne (EPFL), Lausanne, Switzerland*
[42] *Physik-Institut, Universität Zürich, Zürich, Switzerland*
[43] *Nikhef National Institute for Subatomic Physics, Amsterdam, The Netherlands*
[44] *Nikhef National Institute for Subatomic Physics and VU University Amsterdam, Amsterdam, The Netherlands*
[45] *NSC Kharkiv Institute of Physics and Technology (NSC KIPT), Kharkiv, Ukraine*
[46] *Institute for Nuclear Research of the National Academy of Sciences (KINR), Kyiv, Ukraine*
[47] *University of Birmingham, Birmingham, United Kingdom*
[48] *H.H. Wills Physics Laboratory, University of Bristol, Bristol, United Kingdom*
[49] *Cavendish Laboratory, University of Cambridge, Cambridge, United Kingdom*
[50] *Department of Physics, University of Warwick, Coventry, United Kingdom*
[51] *STFC Rutherford Appleton Laboratory, Didcot, United Kingdom*
[52] *School of Physics and Astronomy, University of Edinburgh, Edinburgh, United Kingdom*
[53] *School of Physics and Astronomy, University of Glasgow, Glasgow, United Kingdom*
[54] *Oliver Lodge Laboratory, University of Liverpool, Liverpool, United Kingdom*
[55] *Imperial College London, London, United Kingdom*
[56] *School of Physics and Astronomy, University of Manchester, Manchester, United Kingdom*
[57] *Department of Physics, University of Oxford, Oxford, United Kingdom*
[58] *Massachusetts Institute of Technology, Cambridge, MA, United States*
[59] *University of Cincinnati, Cincinnati, OH, United States*

JHEP01(2018)138

[60] *University of Maryland, College Park, MD, United States*
[61] *Syracuse University, Syracuse, NY, United States*
[62] *Pontifícia Universidade Católica do Rio de Janeiro (PUC-Rio), Rio de Janeiro, Brazil, associated to* [2]
[63] *University of Chinese Academy of Sciences, Beijing, China, associated to* [3]
[64] *School of Physics and Technology, Wuhan University, Wuhan, China, associated to* [3]
[65] *Institute of Particle Physics, Central China Normal University, Wuhan, Hubei, China, associated to* [3]
[66] *Departamento de Fisica , Universidad Nacional de Colombia, Bogota, Colombia, associated to* [8]
[67] *Institut für Physik, Universität Rostock, Rostock, Germany, associated to* [12]
[68] *National Research Centre Kurchatov Institute, Moscow, Russia, associated to* [32]
[69] *National Research Tomsk Polytechnic University, Tomsk, Russia, associated to* [32]
[70] *Instituto de Fisica Corpuscular, Centro Mixto Universidad de Valencia - CSIC, Valencia, Spain, associated to* [38]
[71] *Van Swinderen Institute, University of Groningen, Groningen, The Netherlands, associated to* [43]
[72] *Los Alamos National Laboratory (LANL), Los Alamos, United States, associated to* [61]

[a] *Universidade Federal do Triângulo Mineiro (UFTM), Uberaba-MG, Brazil*
[b] *Laboratoire Leprince-Ringuet, Palaiseau, France*
[c] *P.N. Lebedev Physical Institute, Russian Academy of Science (LPI RAS), Moscow, Russia*
[d] *Università di Bari, Bari, Italy*
[e] *Università di Bologna, Bologna, Italy*
[f] *Università di Cagliari, Cagliari, Italy*
[g] *Università di Ferrara, Ferrara, Italy*
[h] *Università di Genova, Genova, Italy*
[i] *Università di Milano Bicocca, Milano, Italy*
[j] *Università di Roma Tor Vergata, Roma, Italy*
[k] *Università di Roma La Sapienza, Roma, Italy*
[l] *AGH - University of Science and Technology, Faculty of Computer Science, Electronics and Telecommunications, Kraków, Poland*
[m] *LIFAELS, La Salle, Universitat Ramon Llull, Barcelona, Spain*
[n] *Hanoi University of Science, Hanoi, Vietnam*
[o] *Università di Padova, Padova, Italy*
[p] *Università di Pisa, Pisa, Italy*
[q] *Università degli Studi di Milano, Milano, Italy*
[r] *Università di Urbino, Urbino, Italy*
[s] *Università della Basilicata, Potenza, Italy*
[t] *Scuola Normale Superiore, Pisa, Italy*
[u] *Università di Modena e Reggio Emilia, Modena, Italy*
[v] *Iligan Institute of Technology (IIT), Iligan, Philippines*
[w] *Novosibirsk State University, Novosibirsk, Russia*
[†] *Deceased*

JHEP01(2018)138